Recent progress and open problems in the field of exclusive, diffractive and electromagnetic processes

Antoni Szczurek
Institute of Nuclear Physics (PAN), Cracow, Poland
Rzeszów University, Rzeszów, Poland

Diffractive and electromagnetic processes at high energies
Bad Honnef, Germany, August 17-21, 2015

Single diffractive production

- single diffractive dijets
- single diffractive $W^{\pm}$
- single diffractive jet+photon
- single diffractive $c\bar{c}$ or charmed mesons
- single diffractive $b\bar{b}$
- single diffractive J/ψ
- single diffractive $l^{+}l^{-}$
- single diffractive H
- single diffractive $W^{+}W^{-}$

Single diffractive production

- central diffractive dijets
- central diffractive $W^{\pm}$
- central diffractive $c\bar{c}$

Exclusive processes

- $pp \to pp\rho^0, \omega, \phi$
- $pp \to ppJ/\psi, \psi', \Upsilon$ (saturation)
- $pp \to ppH$
- $pp \to ppc\bar{c}$
- $pp \to ppb\bar{b}$, background to Higgs
- $pp \to ppW^+W^-$, anomalous couplings
- $pp \to ppH^+H^-$ (FCC?)
- $pp \to pp\gamma\gamma$, KMR and $\gamma\gamma \to \gamma\gamma$
- $pp \to ppl^+l^-$, $\gamma\gamma$ and exclusive Drell Yan
- $pp \to pp\gamma$ (RHIC?)
- $pp \to ppZ^0$ (upper limit)
- $pp \to pp\pi^0$ (ALICE?)
- $pp \to pn\pi^+$ (ALICE?)

Exclusive reactions

- $pp \to pp\eta$
- $pp \to pp\pi^0(\to \gamma\gamma)(technipion)$
- $pp \to pp\chi_c(0), \chi_c(1), \chi_c(2)$
- $pp \to pp\pi^+\pi^-$, search for glueballs
- $pp \to ppK^+K^-$
- $pp \to pp\rho^0\rho^0$ or $pp\pi^+\pi^-\pi^+\pi^-$
- $pp \to ppp\bar{p}$
- $pp \to ppJ/\psi J/\psi$, BL pQCD mechanism
- semi-exclusive processes with proton excitation and dissociation

Ultraperipheral collisions in heavy ion collisions

- $AA \longrightarrow AA\pi\pi$
- $AA \longrightarrow AA\rho^0$
- $AA \longrightarrow AAJ/\psi$
- $AA \longrightarrow AA\rho^0\rho^0$ ($\gamma\gamma$ and double scattering)
- $AA \longrightarrow AAJ/\psi J/\psi$ (only $\gamma\gamma$)
- $AA \longrightarrow AA\gamma\gamma$, $\gamma\gamma \to \gamma\gamma$
- Semi-central photoproduction collisions
- Electromagnetic dissociation of nuclei (neutron emissions)

Diffractive charm production

Resolved pomeron model (Ingelman-Schlein model)

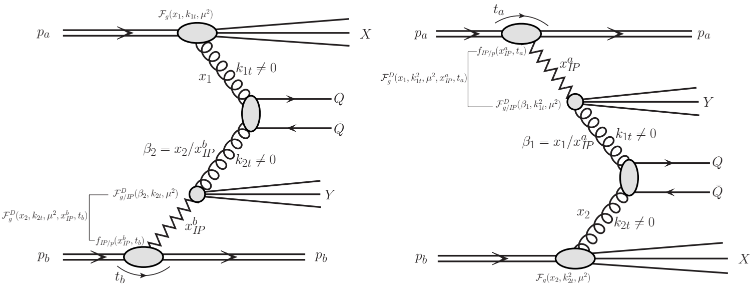

recently very detailed studies in collinear approach:

Luszczak, Maciula, Szczurek, Phys. Rev. **D91** (2015) 054024.

Diffractive charm production

TABLE I: Integrated cross sections for diffractive production of open charm and bottom mesons in different measurement modes for ATLAS, LHCb and CMS experiments at $\sqrt{s} = 14$ TeV.

Acceptance	Mode	Integrated cross sections, [nb]		
		single-diffractive	central-diffractive	non-diffractive EXP data
ATLAS, $\|y\| < 2.5$ $p_\perp > 3.5$ GeV	$D^0 + \overline{D^0}$	$3555.22\ (IR: 25\%)$	$177.35\ (IR: 43\%)$	–
LHCb, $2 < y < 4.5$ $p_\perp < 8$ GeV	$D^0 + \overline{D^0}$	$31442.8\ (IR: 31\%)$	$2526.7\ (IR: 50\%)$	1488000 ± 182000
CMS, $\|y\| < 2.4$ $p_\perp > 5$ GeV	$(B^+ + B^-)/2$	$349.18\ (IR: 24\%)$	$14.24\ (IR: 42\%)$	$28100 \pm 2400 \pm 2000$
LHCb, $2 < y < 4.5$ $p_\perp < 40$ GeV	$B^+ + B^-$	$867.62\ (IR: 27\%)$	$31.03\ (IR: 43\%)$	$41400 \pm 1500 \pm 3100$
LHCb, $2 < y < 4$ $3 < p_\perp < 12$ GeV	$D^0\overline{D^0}$	$179.4\ (IR: 28\%)$	$7.67\ (IR: 45\%)$	$6230 \pm 120 \pm 230$

- single-diffraction: $\frac{R}{P+R} \approx 24 - 31\%$
- central-diffraction: $\frac{PR+RP+RR}{PP+PR+RP+RR} \approx 42 - 50\%$
- $\frac{single-diffractive}{non-diffractive} \approx 2 - 3\%$ $\frac{central-diffractive}{non-diffractive} \approx 0.03 - 0.07\%$

Diffractive charm production

Generalize the collinear approach.

How to calculate diffractive UGDFs?

- 1) take: $g(\beta, \mu^2)$, $q_f(\beta, \mu^2)$ in the pomeron, reggeon known from HERA
- 2) calculate diffractive PDFs: $g^D(x, k_t^2)$, $q_f^D(x, k_t^2)$
- 3) use KMR method: g^D, q_f^D, $\bar{q}_f^D \to \mathcal{F}^D(x, k_t^2, \mu^2)$

Diffractive charm production

Within the k_t-factorization approach

$$d\sigma^{SD(a)}(p_a p_b \to p_a c\bar{c}\, XY) = \int dx_1 \frac{d^2k_{1t}}{\pi} dx_2 \frac{d^2k_{2t}}{\pi}\, dx_{\mathbf{P}}^a\, dt_a\, d\hat{\sigma}(g^* g^* \to c\bar{c}) \times \mathcal{F}_g^D(x_1, k_{1t}^2, \mu^2, x_{\mathbf{P}}^a, t_a) \cdot \mathcal{F}_g(x_2, k_{2t}^2, \mu^2), \quad (1)$$

$$d\sigma^{SD(b)}(p_a p_b \to c\bar{c} p_b\, XY) = \int dx_1 \frac{d^2k_{1t}}{\pi} dx_2 \frac{d^2k_{2t}}{\pi}\, dx_{\mathbf{P}}^b\, dt_b\, d\hat{\sigma}(g^* g^* \to c\bar{c}) \times \mathcal{F}_g(x_1, k_{1t}^2, \mu^2) \cdot \mathcal{F}_g^D(x_2, k_{2t}^2, \mu^2, x_{\mathbf{P}}^b, t_b), \quad (2)$$

where $\mathcal{F}_g(x, k_t^2, \mu^2)$ are the "conventional" UGDFs in and $\mathcal{F}_g^D(x, k_t^2, \mu^2, x_{\mathbf{P}}, t)$ are diffractive UGDFs.

Diffractive charm production

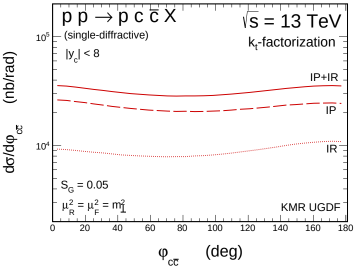

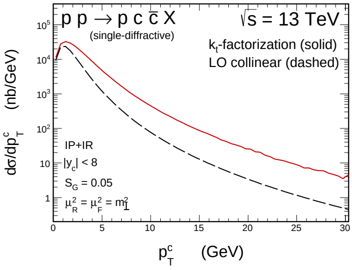

Diffractive charm production

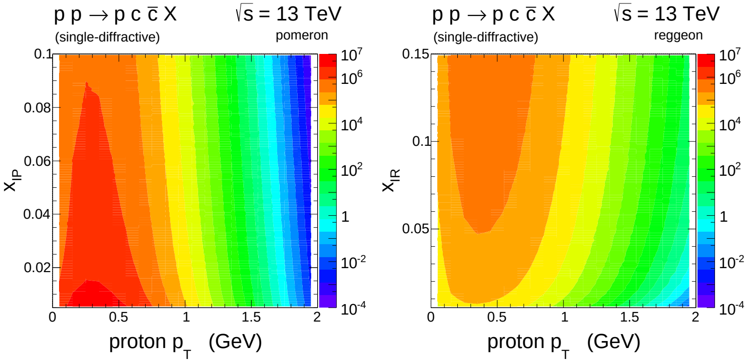

Diffractive charm production

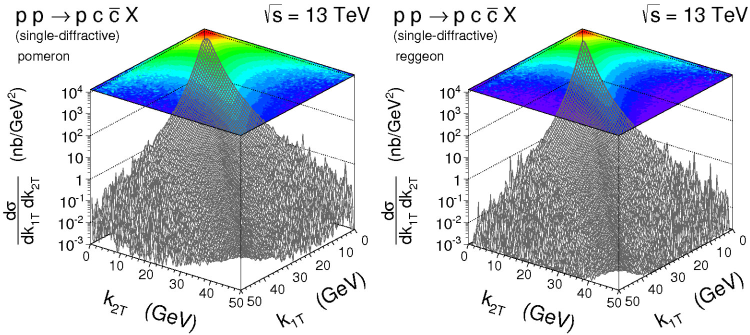

broad distributions

Single diffractive production

- Something concrete must be measured at the LHC to verify our understanding of single diffractive production

$pp \to pp\pi^+\pi^-$

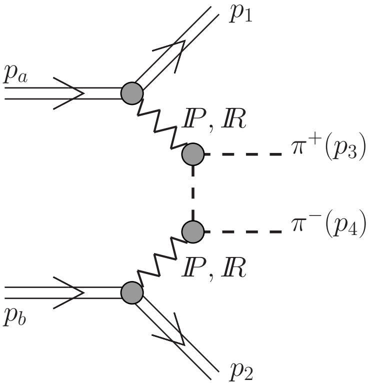

On theoretical side only continuum with absorption
(Durham and Kraków)

$pp \to pp\pi^+\pi^-$

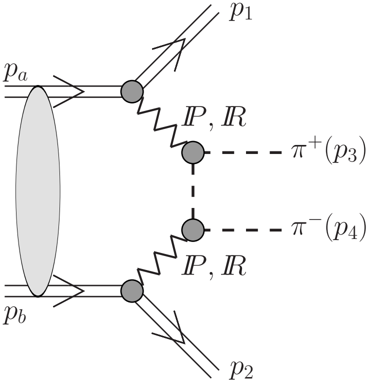

nucleon-nucleon interaction

$pp \to pp\pi^+\pi^-$

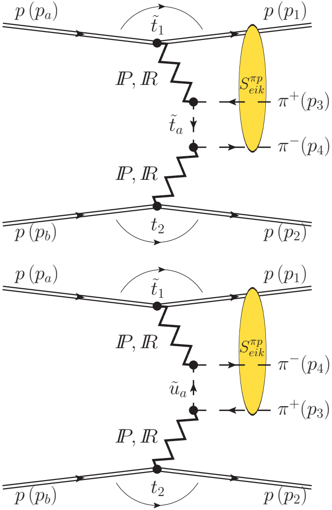

$p\,(p_a)$
$p\,(p_1)$
$\tilde{t}_1$
$I\!P, I\!R$
$S^{\pi p}_{eik}$
$\pi^+(p_3)$
$\tilde{t}_a$
$\pi^-(p_4)$
$I\!P, I\!R$
t_2
$p\,(p_b)$
$p\,(p_2)$
$p\,(p_a)$
$p\,(p_1)$
t_1
$I\!P, I\!R$
$\pi^+(p_3)$
$\tilde{t}_b$
$\pi^-(p_4)$
$S^{\pi p}_{eik}$
$I\!P, I\!R$
$\tilde{t}_2$
$p\,(p_b)$
$p\,(p_2)$
$p\,(p_a)$
$p\,(p_1)$
$\tilde{t}_1$
$I\!P, I\!R$
$S^{\pi p}_{eik}$
$\pi^-(p_4)$
$\tilde{u}_a$
$\pi^+(p_3)$
$I\!P, I\!R$
t_2
$p\,(p_b)$
$p\,(p_2)$
$p\,(p_a)$
$p\,(p_1)$
t_1
$I\!P, I\!R$
$\pi^-(p_4)$
$\tilde{u}_b$
$\pi^+(p_3)$
$S^{\pi p}_{eik}$
$I\!P, I\!R$
$\tilde{t}_2$
$p\,(p_b)$
$p\,(p_2)$

$pp \to pp\pi^+\pi^-$

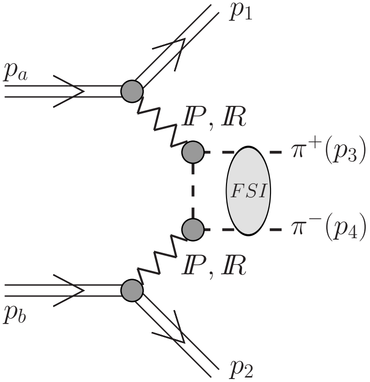

$\pi\pi$ FSI low-energy effects have to be included

$pp \to pp\pi^+\pi^-$

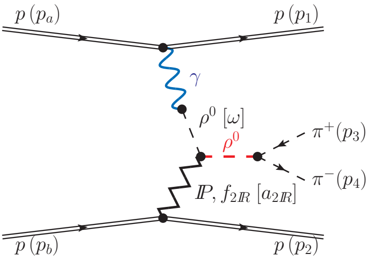

Different C-parity of $\pi\pi$

Quite sizeable contribution

$pp \to pp\pi^+\pi^-$

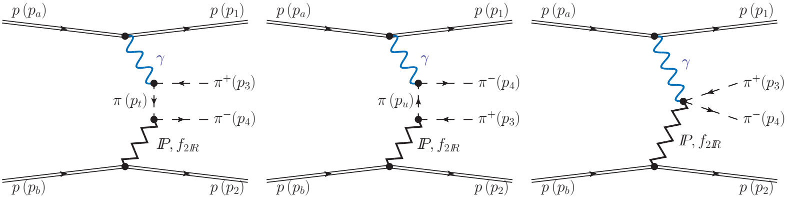

Different C-parity of $\pi\pi$

$pp \to pp\pi^+\pi^-$

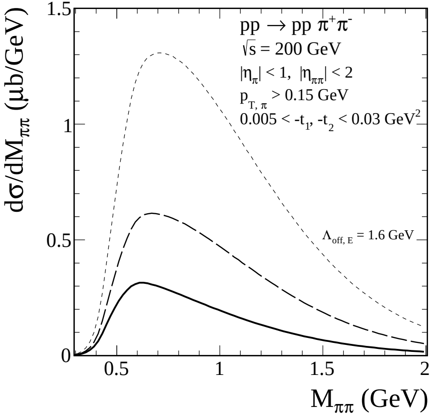

Strong new absorption effects

Similar situation for CDF, ALICE. etc.

$pp \to pp\pi^+\pi^-$

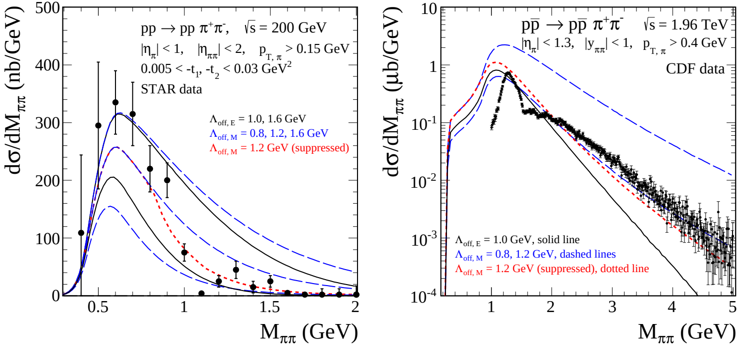

preliminary STAR data

Impossible to describe both STAR and CDF data at least with the present ingredients.

$pp \to pp\pi^+\pi^-$

Suggestions for theoretical calculations:

- Inclusion of continuum and resonances ($f_0(980)$, $f_2(1270)$), $f_0(1500)$
  in a consistent model seems necessary.
  Tensor pomeron model of Nachtmann et al. is a candidate
- FSI effects
- Include also photoproduction mechanism

Suggestions for experimental analyses:

- Show how the $M_{\pi\pi}$ spectra change when gradually increasing rapidity gaps to clarify exclusivity.
- measure protons (ATLAS and CMS)
- Do the experimental acceptance corrections require a theoretical model?

$pp \to ppJ/\psi$

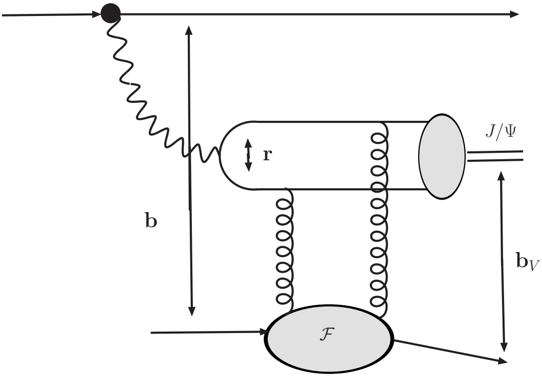

A. Cisek, W. Schäfer and A. Szczurek, JHEP **1504** (2015) 159.

$pp \to ppJ/\psi$

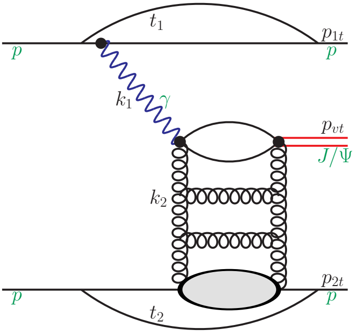

The interference term vanishes for rapidity distributions in Born approximation

see W. Schäfer and A. Szczurek, Phys. Rev. **D76** (2007) 094014.

$pp \to ppJ/\psi$

$$\Im m\,\mathcal{M}_T(W,\Delta^2=0,Q^2=0) = W^2 \frac{c_V\sqrt{4\pi\alpha_{em}}}{4\pi^2}\, 2\int_0^1 \frac{dz}{z(1-z)}\int_0^\infty \pi dk^2 \psi_V(z,k^2)$$
$$\int_0^\infty \frac{\pi d\kappa^2}{\kappa^4}\alpha_S(q^2)\mathcal{F}(x_{\rm eff},\kappa^2)\Big(A_0(z,k^2)\; W_0(k^2,\kappa^2) + A_1(z,k^2)\; W_1(k^2,\kappa^2)\Big). \quad ($$

dependence on the meson wave function and UGDF

No wave functions in collinear calculations.

$pp \to ppJ/\psi$

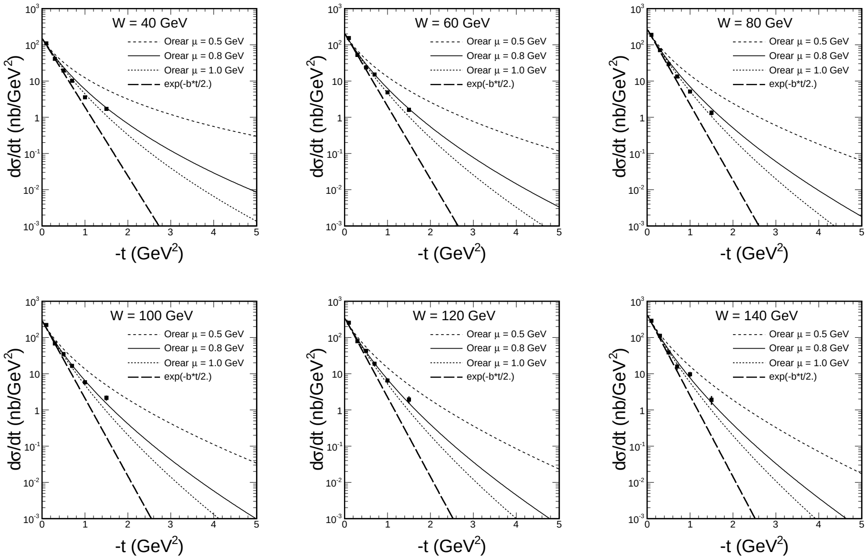

W = 40 GeV
W = 60 GeV
W = 80 GeV
W = 100 GeV
W = 120 GeV
W = 140 GeV
Orear μ = 0.5 GeV
Orear μ = 0.8 GeV
Orear μ = 1.0 GeV
exp(-b*t/2.)
dσ/dt (nb/GeV²)
-t (GeV²)

$pp \to ppJ/\psi$

$$\mathcal{M}^{\lambda_1\lambda_2\to\lambda'_1\lambda'_2\lambda_V}_{h_1h_2\to h_1h_2V}(s,s_1,s_2,t_1,t_2) = \mathcal{M}_{\gamma\mathbf{P}} + \mathcal{M}_{\mathbf{P}\gamma}$$
$$= \langle p'_1,\lambda'_1|J_\mu|p_1,\lambda_1\rangle\epsilon^*_\mu(q_1,\lambda_V)\frac{\sqrt{4\pi\alpha_{em}}}{t_1}\mathcal{M}^{\lambda_{\gamma^*}\lambda_2\to\lambda_V\lambda_2}_{\gamma^*h_2\to Vh_2}(s_2,t_2,Q_1^2)$$
$$+\langle p'_2,\lambda'_2|J_\mu|p_2,\lambda_2\rangle\epsilon^*_\mu(q_2,\lambda_V)\frac{\sqrt{4\pi\alpha_{em}}}{t_2}\mathcal{M}^{\lambda_{\gamma^*}\lambda_1\to\lambda_V\lambda_1}_{\gamma^*h_1\to Vh_1}(s_1,t_1,Q_2^2)\,. \qquad (4)$$

$pp \rightarrow ppJ/\psi$

Then, the amplitude of Eq. (4) for the emission of a photon of transverse polarization λ_V, and transverse momentum $\boldsymbol{q}_1 = -\boldsymbol{p}_1$ can be written as:

$$\begin{aligned} &\langle p_1', \lambda_1' | J_\mu | p_1, \lambda_1 \rangle \epsilon_\mu^*(q_1, \lambda_V) \\ &= \frac{(\boldsymbol{e}^{*(\lambda_V)} \boldsymbol{q}_1)}{\sqrt{1 - z_1}} \, \frac{2}{z_1} \, \chi_{\lambda'}^\dagger \Big\{ F_1(Q_1^2) - \frac{i\kappa_p F_2(Q_1^2)}{2m_p} (\sigma_1 \cdot [\boldsymbol{q}_1, \boldsymbol{n}]) \Big\} \chi_\lambda \, . \end{aligned} \tag{5}$$

$pp \to ppJ/\psi$

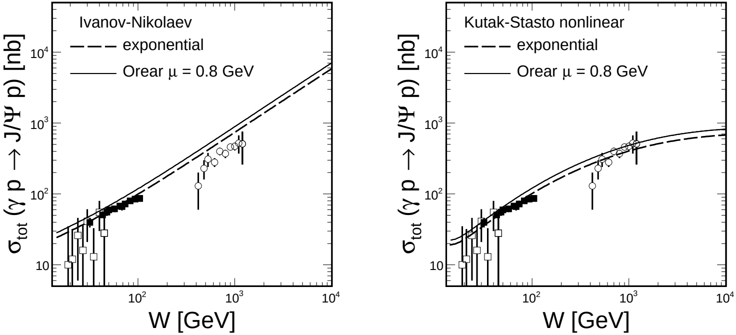

Ivanov-Nikolaev
exponential
Orear μ = 0.8 GeV
Kutak-Stasto nonlinear
exponential
Orear μ = 0.8 GeV
σ_tot (γ p → J/Ψ p) [nb]
W [GeV]

$pp \to ppJ/\psi$

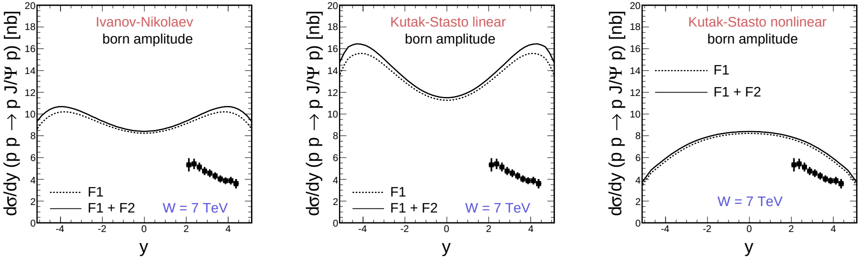
Ivanov-Nikolaev
born amplitude
F1
F1 + F2
W = 7 TeV
Kutak-Stasto linear
born amplitude
F1
F1 + F2
W = 7 TeV
Kutak-Stasto nonlinear
born amplitude
F1
F1 + F2
W = 7 TeV
dσ/dy (p p → p J/Ψ p) [nb]
y

$pp \to ppJ/\psi$

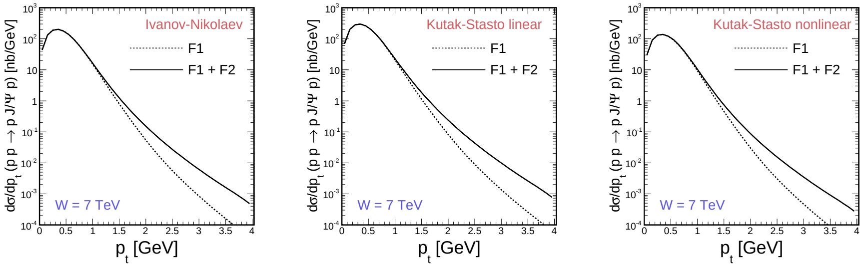

Ivanov-Nikolaev
F1
F1 + F2
W = 7 TeV
Kutak-Stasto linear
F1
F1 + F2
W = 7 TeV
Kutak-Stasto nonlinear
F1
F1 + F2
W = 7 TeV
dσ/dp_t (p p → p J/Ψ p) [nb/GeV]
p_t [GeV]

$pp \to ppJ/\psi$

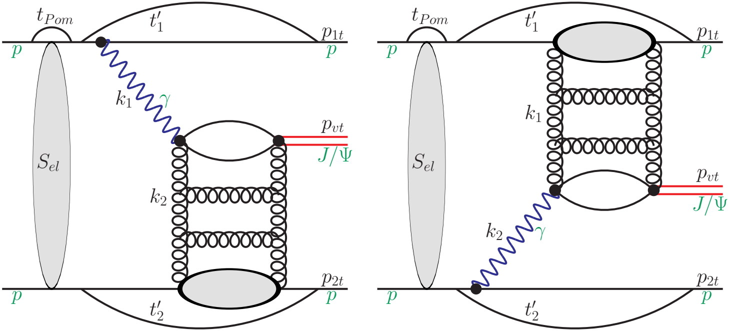

Survival factor depends on the phase space point !

$pp \to ppJ/\psi$

with absorption

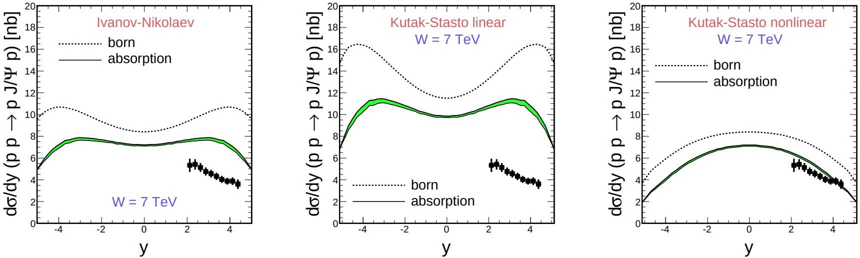

similar for ψ'

$pp \to ppJ/\psi$

with absorption

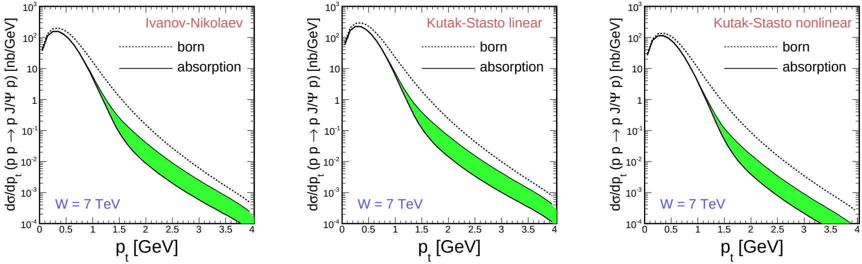

similar for ψ'

$pp \to ppJ/\psi$

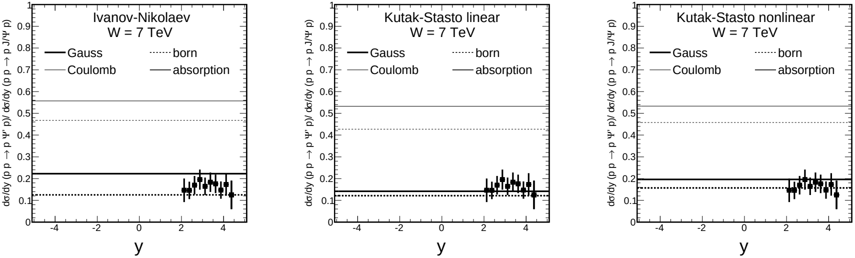

Gauss WF much better than Coulomb WF

$pp \to ppJ/\psi$

There is some model dependent indication of nonlinear effects

Open problems:

- The present experiments are not exclusive.
- So far proton dissociation "extracted" in a model dependent way assuming some functional form in p_t.
- We have some knowledge about diffractive dissociation (HERA).
- Compare to HERA there is also photon dissociation (never discussed, probably bigger).
- Interference effects due to the two diagrams were predicted. It would be nice to see modulation in ϕ_{pp} due to interference effects between the two diagrams.
- CMS+TOTEM and ATLAS+ALFA could measure purely exclusive reaction and study dependences on many more variables.

$pp \to l^+l^-$

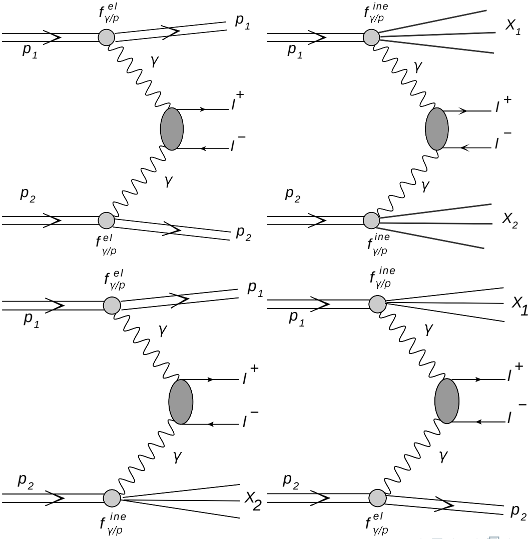

f el γ/p
p 1
p 1
γ
l +
l −
γ
p 2
p 2
f el γ/p
f ine γ/p
X 1
p 1
γ
l +
l −
γ
p 2
X 2
f ine γ/p
f el γ/p
p 1
p 1
γ
l +
l −
γ
p 2
X 2
f ine γ/p
f ine γ/p
X 1
p 1
γ
l +
l −
γ
p 2
p 2
f el γ/p

$pp \to l^+ l^-$

Two different approach are possible:
- collinear - factorization:
(M. Łuszczak, A. Szczurek and Ch. Royon, JHEP 1502 (2015) 098, arXiv:1409.1803)
- k_t - factorization
(G. Gil da Silveira, L. Forthomme, K. Piotrzkowski, W. Schafer, A. Szczurek, JHEP 1502 (2015) 159,
M. Luszczak, W. Schafer and A. Szczurek, work in progress)

In collinear - factorization approach one needs photons as parton in proton:
- MRST
- NNPDF

MRST parton distributions

The factorization of the QED-induced collinear divergences leads to QED-corrected evolution equations for the parton distributions of the proton.

$$
\begin{aligned}
\frac{\partial q_i(x,\mu^2)}{\partial \log \mu^2} &= \frac{\alpha_S}{2\pi}\int_x^1 \frac{dy}{y}\left\{P_{qq}(y)\; q_i\left(\frac{x}{y},\mu^2\right) + P_{qg}(y)\; g\left(\frac{x}{y},\mu^2\right)\right\} \\
&+ \frac{\alpha}{2\pi}\int_x^1 \frac{dy}{y}\left\{\tilde{P}_{qq}(y)\; e_i^2 q_i\left(\frac{x}{y},\mu^2\right) + P_{q\gamma}(y)\; e_i^2 \gamma\left(\frac{x}{y},\mu^2\right)\right\} \\
\frac{\partial g(x,\mu^2)}{\partial \log \mu^2} &= \frac{\alpha_S}{2\pi}\int_x^1 \frac{dy}{y}\left\{P_{gq}(y)\; \sum_j q_j\left(\frac{x}{y},\mu^2\right) + P_{gg}(y)\; g\left(\frac{x}{y},\mu^2\right)\right\} \\
\frac{\partial \gamma(x,\mu^2)}{\partial \log \mu^2} &= \frac{\alpha}{2\pi}\int_x^1 \frac{dy}{y}\left\{P_{\gamma q}(y)\; \sum_j e_j^2\; q_j\left(\frac{x}{y},\mu^2\right) + P_{\gamma\gamma}(y)\; \gamma\left(\frac{x}{y},\mu^2\right)\right\},
\end{aligned}
$$

$pp \to l^+ l^-$

Collinear photon distribution in nucleon

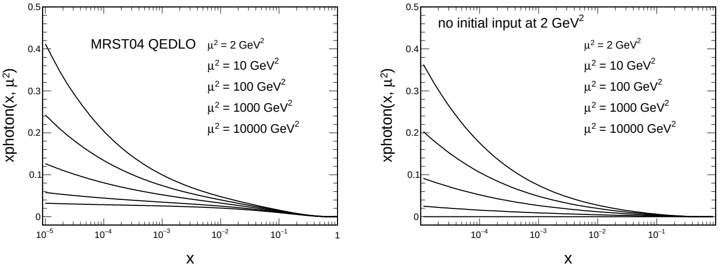

initial input is crucial

$pp \to l^+ l^-$

$$\frac{d\sigma^{\gamma_{in}\gamma_{in}}}{dy_1 dy_2 d^2p_t} = \frac{1}{16\pi^2\hat{s}^2} x_1\gamma_{in}(x_1,\mu^2)\; x_2\gamma_{in}(x_2,\mu^2)\; \overline{|\mathcal{M}_{\gamma\gamma\to W^+W^-}|^2}$$

$$\frac{d\sigma^{\gamma_{in}\gamma_{el}}}{dy_1 dy_2 d^2p_t} = \frac{1}{16\pi^2\hat{s}^2} x_1\gamma_{in}(x_1,\mu^2)\; x_2\gamma_{el}(x_2,\mu^2)\; \overline{|\mathcal{M}_{\gamma\gamma\to W^+W^-}|^2}$$

$$\frac{d\sigma^{\gamma_{el}\gamma_{in}}}{dy_1 dy_2 d^2p_t} = \frac{1}{16\pi^2\hat{s}^2} x_1\gamma_{el}(x_1,\mu^2)\; x_2\gamma_{in}(x_2,\mu^2)\; \overline{|\mathcal{M}_{\gamma\gamma\to W^+W^-}|^2}$$

$$\frac{d\sigma^{\gamma_{el}\gamma_{el}}}{dy_1 dy_2 d^2p_t} = \frac{1}{16\pi^2\hat{s}^2} x_1\gamma_{el}(x_1,\mu^2)\; x_2\gamma_{el}(x_2,\mu^2)\; \overline{|\mathcal{M}_{\gamma\gamma\to W^+W^-}|^2}$$

The elastic photon fluxes are calculated using the Drees-Zeppenfeld parametrization, where a simple parametrization of nucleon electromagnetic form factors was used

$pp \to l^+ l^-$

$$\mathcal{F}_{\gamma^* \leftarrow A}(z, \boldsymbol{q}) = \frac{\alpha_{\rm em}}{\pi}\,(1-z)\left(\frac{\boldsymbol{q}^2}{\boldsymbol{q}^2 + z(M_X^2 - m_A^2) + z^2 m_A^2}\right)^2 \cdot \frac{p_B^\mu p_B^\nu}{s^2}\, W_{\mu\nu}(M_X^2, Q^2$$

The hadronic tensor is expressed in terms of the electromagnetic currents as:

$$W_{\mu\nu}(M_X^2, Q^2) = \overline{\sum_X} (2\pi)^3\, \delta^{(4)}(p_X - p_A - q)\, \langle p | J_\mu | X \rangle \langle X | J_\nu^\dagger | p \rangle\, d\Phi_X\,, \quad (7)$$

$$W_{\mu\nu}(M_X^2, Q^2) = -\delta^{\perp}_{\mu\nu}(p_A, q)\, W_T(M_X^2, Q^2) + e_\mu^{(0)} e_\nu^{(0)}\, W_L(M_X^2, Q^2)\,. \quad (8)$$

The virtual photoabsorption cross sections are defined as

$$\sigma_T(\gamma^* p) = \frac{4\pi\alpha_{em}}{4\sqrt{X}}\Big(-\frac{\delta^{\perp}_{\mu\nu}}{2}\Big) 2\pi W^{\mu\nu}(M_X^2, Q^2)$$
$$\sigma_L(\gamma^* p) = \frac{4\pi\alpha_{em}}{4\sqrt{X}}\, e_\mu^0 e_\nu^0\, 2\pi W^{\mu\nu}(M_X^2, Q^2)\,. \quad (9)$$

It is customary to introduce dimensionless structure function $F_i(x_{\rm Bj}, Q^2), i = T, L$ as

$$\sigma_{T,L}(\gamma^* p) = \frac{4\pi^2\alpha_{em}}{Q^2}\,\frac{1}{\sqrt{1 + \frac{4x_{\rm Bj}^2 m_A^2}{Q^2}}}\, F_{T,L}(x_{\rm Bj}, Q^2)\,, \quad (10)$$

In the literature one often finds structure functions $F_1(x_{\rm Bj}, Q^2), F_2(x_{\rm Bj}, Q^2)$, which are related to $F_{T,L}$ through

$pp \to l^+ l^-$

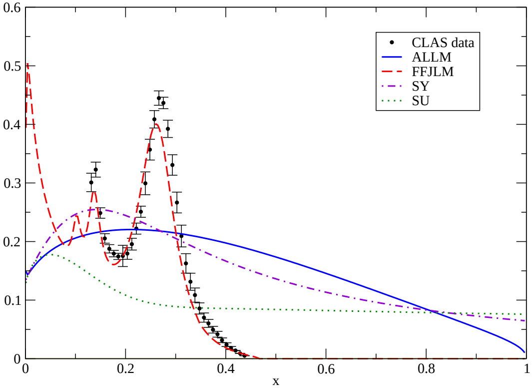

$pp \to l^+ l^-$

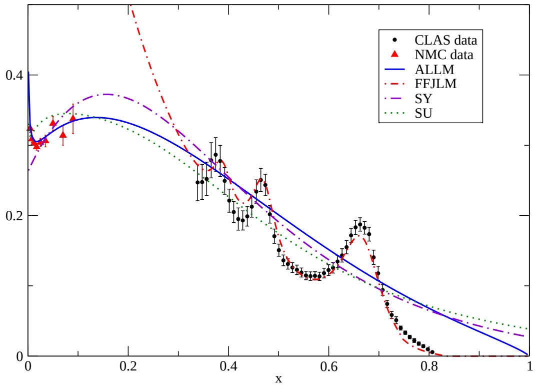

$pp \to l^+l^-$

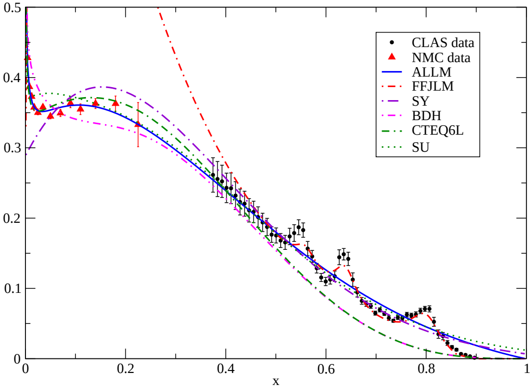

CLAS data
NMC data
ALLM
FFJLM
SY
BDH
CTEQ6L
SU
x
0
0.2
0.4
0.6
0.8
1
0.1
0.2
0.3
0.4
0.5

$pp \to l^+ l^-$

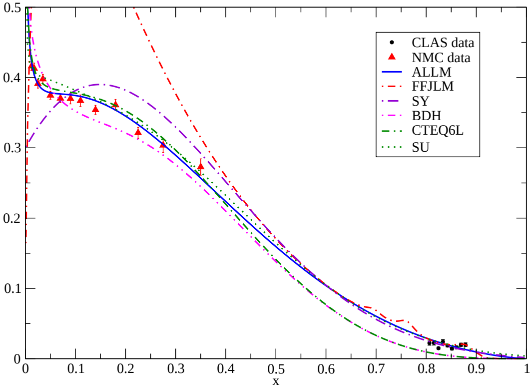
0.5
0.4
0.3
0.2
0.1
0
0
0.1
0.2
0.3
0.4
0.5
0.6
0.7
0.8
0.9
1
x
CLAS data
NMC data
ALLM
FFJLM
SY
BDH
CTEQ6L
SU

$pp \to l^+ l^-$

k_t-factorization, including photon transverse momenta

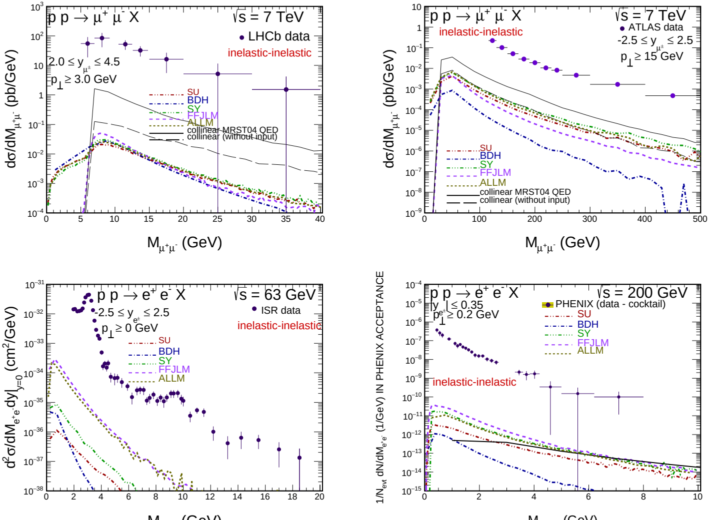

$pp \to l^+ l^-$

k_t-factorization, including photon transverse momenta

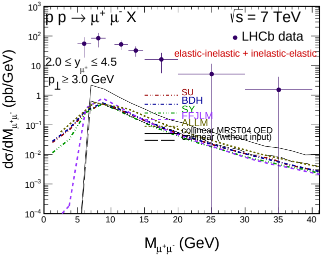

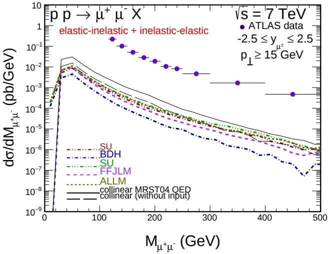

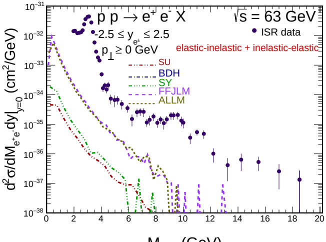

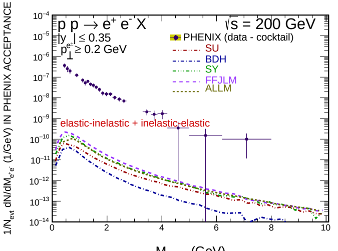

$pp \to l^+ l^-$

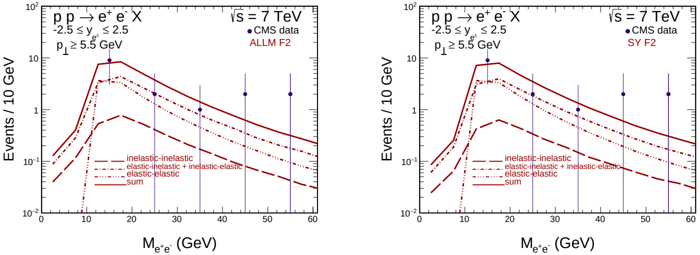
p p → e+ e- X
-2.5 ≤ y ≤ 2.5
p⊥ ≥ 5.5 GeV
√s = 7 TeV
CMS data
ALLM F2
inelastic-inelastic
elastic-inelastic + inelastic-elastic
elastic-elastic
sum
Events / 10 GeV
M (GeV)
p p → e+ e- X
-2.5 ≤ y ≤ 2.5
p⊥ ≥ 5.5 GeV
√s = 7 TeV
CMS data
SY F2
inelastic-inelastic
elastic-inelastic + inelastic-elastic
elastic-elastic
sum
Events / 10 GeV
M (GeV)

$pp \to l^+ l^-$

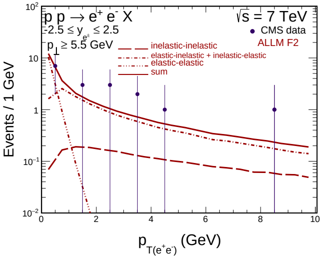
p p → e+ e- X
-2.5 ≤ y ≤ 2.5
p⊥ ≥ 5.5 GeV
√s = 7 TeV
CMS data
ALLM F2
inelastic-inelastic
elastic-inelastic + inelastic-elastic
elastic-elastic
sum
Events / 1 GeV
p T(e+e-) (GeV)

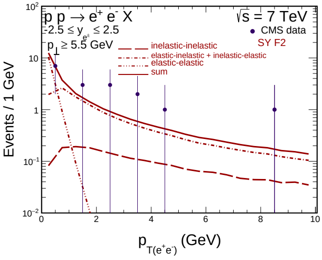
p p → e+ e- X
-2.5 ≤ y ≤ 2.5
p⊥ ≥ 5.5 GeV
√s = 7 TeV
CMS data
SY F2
inelastic-inelastic
elastic-inelastic + inelastic-elastic
elastic-elastic
sum
Events / 1 GeV
p T(e+e-) (GeV)

$pp \rightarrow l^+ l^-$

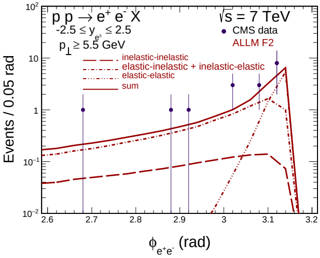

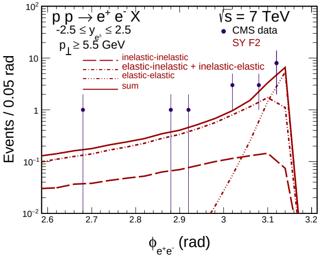

$pp \to W^+W^-$

- Inclusive cross section for W^+W^- production in proton-proton scattering was measured by the ATLAS and CMS collaborations.
- The cross section was calculated at NLO collinear approach (some missing strength ?)
- Many processes are not included in the so-called Standard Model approach
- Production of W^+W^- with no activity close to μ^+e^- or μ^-e^+ vertices was measured by the CMS and recently by ATLAS.
- It was argued that inclusive W^+W^- cross section could be described via double-parton scattering mechanism and competes with the $H \to W^{*,+}W^-, W^{*,-}W^+$

$pp \to W^+W^-$

- The exclusive $pp \to ppW^+W^-$ reaction is particularly interesting in the context of $\gamma\gamma WW$ coupling
- The general diagram for the $pp \to ppW^+W^-$ reaction via $\gamma_{el}\gamma_{el} \to W^+W^-$*subprocess*

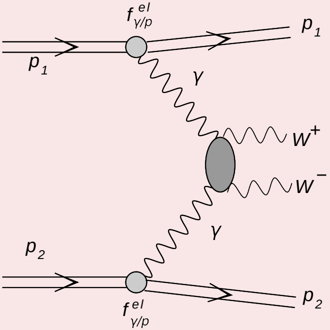

$pp \rightarrow W^+W^-$

The three-boson $WW\gamma$ and four-boson $WW\gamma\gamma$ couplings, which contribute to the $\gamma\gamma \rightarrow W^+W^-$ process in the leading order:

$$\mathcal{L}_{WW\gamma} = -ie(A_\mu W_\nu^- \mu W^{+\nu} + W_\mu^- W_\nu^+ \mu A^\nu + W_\mu^+ A_\nu \mu W^{-\nu}) ,$$

$$\mathcal{L}_{WW\gamma\gamma} = -e^2(W_\mu^- W^{+\mu} A_\nu A^\nu - W_\mu^- A^\mu W_\nu^+ A^\nu) ,$$

where the asymmetric derivative has the form $X\mu Y = X\partial^\mu Y - Y\partial^\mu X$.

- The Born diagrams for the $\gamma\gamma \to W^+W^-$ subprocess

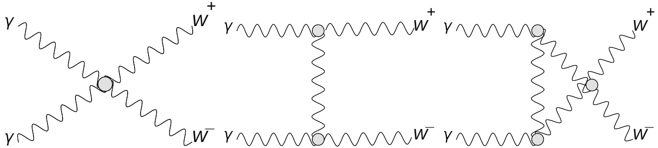

$pp \to W^+W^-$

The elementary tree-level cross section for the $\gamma\gamma \to W^+W^-$ subprocess can be written in the compact form in terms of the Mandelstam variables

$$\frac{d\hat{\sigma}}{d\Omega} = \frac{3\alpha^2\beta}{2\hat{s}}\left(1 - \frac{2\hat{s}(2\hat{s}+3m_W^2)}{3(m_W^2-\hat{t})(m_W^2-\hat{u})} + \frac{2\hat{s}^2(\hat{s}^2+3m_W^4)}{3(m_W^2-\hat{t})^2(m_W^2-\hat{u})^2}\right),$$

$\beta = \sqrt{1-4m_W^2/\hat{s}}$ is the velocity of the W bosons in their center-of-mass frame and the electromagnetic fine-structure constant $\alpha = e^2/(4\pi) \simeq 1/137$ for the on-shell photon

Exclusive diffractive mechanism

The exclusive diffractive KMR mechanism of central production of W^+W^- pairs in proton-proton collisions at the LHC (in which diagrams with intermediate virtual Higgs boson as well as quark box diagrams are included) was discussed in

- P. Lebiedowicz, R. Pasechnik and A. Szczurek, Phys. Rev. **D81** (2012) 036003

and turned out to be negligibly small.

$pp \to W^+W^-$

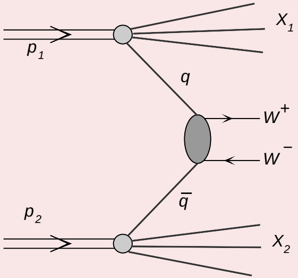

Relevant leading-order matrix element, averaged over quark colors and over initial spin polarizations, summed over final spin polarization and cross section are well known.

$pp \to W^+W^-$

- $\gamma\gamma$ processes contribute also to inclusive cross section. We consider in addition 3 new mechanisms

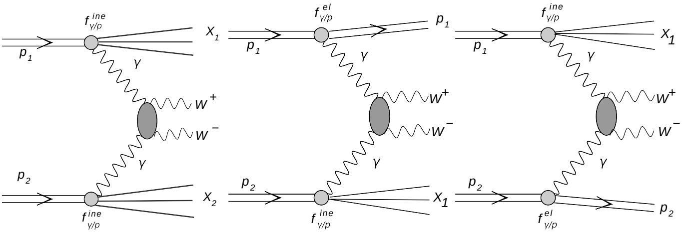

$pp \to W^+W^-$

$$\frac{d\sigma^{\gamma_{in}\gamma_{in}}}{dy_1\,dy_2\,d^2p_t} = \frac{1}{16\pi^2\hat{s}^2} x_1\gamma_{in}(x_1,\mu^2)\; x_2\gamma_{in}(x_2,\mu^2)\; \overline{|\mathcal{M}_{\gamma\gamma\to W^+W^-}|^2}$$

$$\frac{d\sigma^{\gamma_{in}\gamma_{el}}}{dy_1\,dy_2\,d^2p_t} = \frac{1}{16\pi^2\hat{s}^2} x_1\gamma_{in}(x_1,\mu^2)\; x_2\gamma_{el}(x_2,\mu^2)\; \overline{|\mathcal{M}_{\gamma\gamma\to W^+W^-}|^2}$$

$$\frac{d\sigma^{\gamma_{el}\gamma_{in}}}{dy_1\,dy_2\,d^2p_t} = \frac{1}{16\pi^2\hat{s}^2} x_1\gamma_{el}(x_1,\mu^2)\; x_2\gamma_{in}(x_2,\mu^2)\; \overline{|\mathcal{M}_{\gamma\gamma\to W^+W^-}|^2}$$

$$\frac{d\sigma^{\gamma_{el}\gamma_{el}}}{dy_1\,dy_2\,d^2p_t} = \frac{1}{16\pi^2\hat{s}^2} x_1\gamma_{el}(x_1,\mu^2)\; x_2\gamma_{el}(x_2,\mu^2)\; \overline{|\mathcal{M}_{\gamma\gamma\to W^+W^-}|^2}$$

The elastic photon fluxes are calculated using the Drees-Zeppenfeld parametrization, where a simple parametrization of nucleon electromagnetic form factors was used

$pp \to W^+W^-$

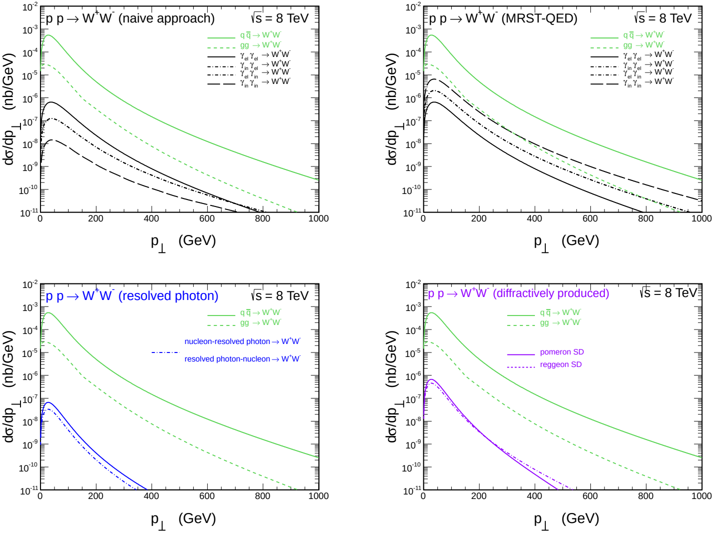
p p → W⁺W⁻ (naive approach)
√s = 8 TeV
q q̄ → W⁺W⁻
gg → W⁺W⁻
γel γel → W⁺W⁻
γin γel → W⁺W⁻
γel γin → W⁺W⁻
γin γin → W⁺W⁻
dσ/dp⊥ (nb/GeV)
p⊥ (GeV)
p p → W⁺W⁻ (MRST-QED)
√s = 8 TeV
q q̄ → W⁺W⁻
gg → W⁺W⁻
γel γel → W⁺W⁻
γin γel → W⁺W⁻
γel γin → W⁺W⁻
γin γin → W⁺W⁻
dσ/dp⊥ (nb/GeV)
p⊥ (GeV)
p p → W⁺W⁻ (resolved photon)
√s = 8 TeV
q q̄ → W⁺W⁻
gg → W⁺W⁻
nucleon-resolved photon → W⁺W⁻
resolved photon-nucleon → W⁺W⁻
dσ/dp⊥ (nb/GeV)
p⊥ (GeV)
p p → W⁺W⁻ (diffractively produced)
√s = 8 TeV
q q̄ → W⁺W⁻
gg → W⁺W⁻
pomeron SD
reggeon SD
dσ/dp⊥ (nb/GeV)
p⊥ (GeV)

$pp \to W^+W^-$

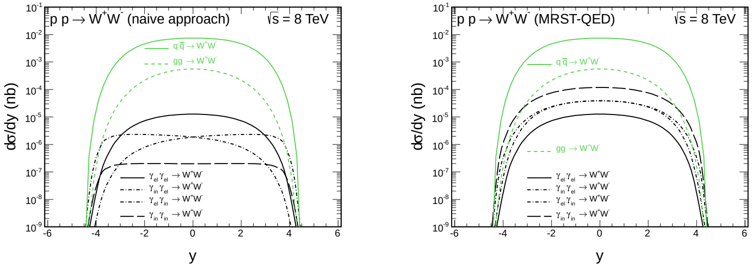

p p → W+W- (naive approach)
√s = 8 TeV
q q̄ → W+W-
gg → W+W-
γel γel → W+W-
γin γel → W+W-
γel γin → W+W-
γin γin → W+W-
dσ/dy (nb)
y
p p → W+W- (MRST-QED)
√s = 8 TeV
q q̄ → W+W-
gg → W+W-
γel γel → W+W-
γin γel → W+W-
γel γin → W+W-
γin γin → W+W-
dσ/dy (nb)
y

$pp \to W^+W^-$

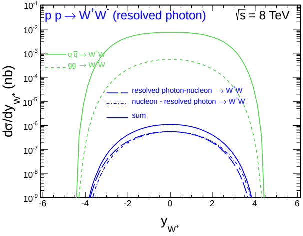

p p → W⁺W⁻ (resolved photon)
√s = 8 TeV
q q̄ → W⁺W⁻
gg → W⁺W⁻
resolved photon-nucleon → W⁺W⁻
nucleon - resolved photon → W⁺W⁻
sum
dσ/dy_{W⁺} (nb)
y_{W⁺}

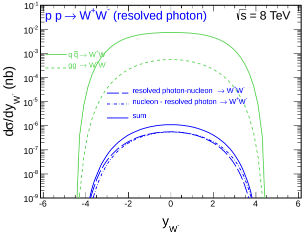

p p → W⁺W⁻ (resolved photon)
√s = 8 TeV
q q̄ → W⁺W⁻
gg → W⁺W⁻
resolved photon-nucleon → W⁺W⁻
nucleon - resolved photon → W⁺W⁻
sum
dσ/dy_{W⁻} (nb)
y_{W⁻}

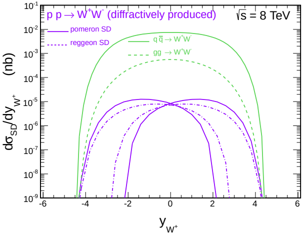

p p → W⁺W⁻ (diffractively produced)
√s = 8 TeV
pomeron SD
reggeon SD
q q̄ → W⁺W⁻
gg → W⁺W⁻
dσ_SD/dy_{W⁺} (nb)
y_{W⁺}

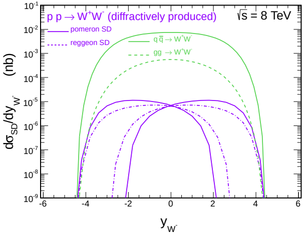

p p → W⁺W⁻ (diffractively produced)
√s = 8 TeV
pomeron SD
reggeon SD
q q̄ → W⁺W⁻
gg → W⁺W⁻
dσ_SD/dy_{W⁻} (nb)
y_{W⁻}

$pp \to W^+W^-$

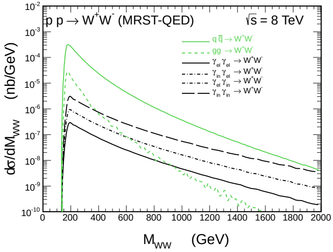
p p → W+W- (MRST-QED)
√s = 8 TeV
q q̄ → W+W-
gg → W+W-
γel γel → W+W-
γin γel → W+W-
γel γin → W+W-
γin γin → W+W-
dσ/dMWW (nb/GeV)
MWW (GeV)

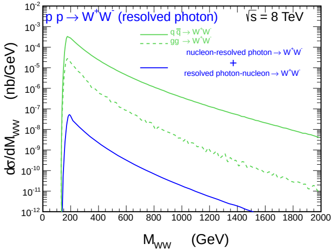
p p → W+W- (resolved photon)
√s = 8 TeV
q q̄ → W+W-
gg → W+W-
nucleon-resolved photon → W+W-
+
resolved photon-nucleon → W+W-
dσ/dMWW (nb/GeV)
MWW (GeV)

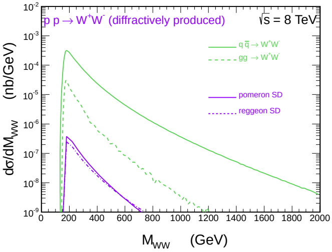
p p → W+W- (diffractively produced)
√s = 8 TeV
q q̄ → W+W-
gg → W+W-
pomeron SD
reggeon SD
dσ/dMWW (nb/GeV)
MWW (GeV)

$pp \to W^+W^-$

contribution	1.96 TeV	7 TeV	8 TeV	14 TeV	comment
CDF	12.1 pb				
D0	13.8 pb				
ATLAS		54.4 pb			large extrapolation
CMS		41.1 pb			large extrapolation
$q\bar{q}$	9.86	27.24	33.04	70.21	dominant (LO, NLO)
gg	$5.17\ 10^{-2}$	1.48	1.97	5.87	subdominant (NLO)
$\gamma_{el}\gamma_{el}$	$3.07\ 10^{-3}$	$4.41\ 10^{-2}$	$5.40\ 10^{-2}$	$1.16\ 10^{-1}$	new, anomalous $\gamma\gamma WW$
$\gamma_{el}\gamma_{in}$	$1.08\ 10^{-2}$	$1.40\ 10^{-1}$	$1.71\ 10^{-1}$	$3.71\ 10^{-1}$	new, anomalous $\gamma\gamma WW$
$\gamma_{in}\gamma_{el}$	$1.08\ 10^{-2}$	$1.40\ 10^{-1}$	$1.71\ 10^{-1}$	$3.71\ 10^{-1}$	new, anomalous $\gamma\gamma WW$
$\gamma_{in}\gamma_{in}$	$3.72\ 10^{-2}$	$4.46\ 10^{-1}$	$5.47\ 10^{-1}$	1.19	anomalous $\gamma\gamma WW$
$\gamma_{el,res} - q/\bar{q}$	$1.04\ 10^{-4}$	$2.94\ 10^{-3}$	$3.83\ 10^{-3}$	$1.03\ 10^{-2}$	new, quite sizeable
$q/\bar{q} - \gamma_{el.res}$	$1.04\ 10^{-4}$	$2.94\ 10^{-3}$	$3.83\ 10^{-3}$	1.0310^{-2}	new, quite sizeable
$\gamma_{in,res} - q/\bar{q}$					new, quite sizeable
$q/\bar{q} - \gamma_{in.res}$					new, quite sizeable
double scattering	$1.2\ 10^{-2}$	0.26	0.36	1.28	not included in NLO studies
$\mathbf{P}p$	$2.82\ 10^{-2}$	$9.88\ 10^{-1}$	1.27	3.35	new, relatively small
$p\mathbf{P}$	$2.82\ 10^{-2}$	$9.88\ 10^{-1}$	1.27	3.35	new, relatively small
$\mathbf{R}p$	$4.51\ 10^{-2}$	$7.12\ 10^{-1}$	$8.92\ 10^{-1}$	2.22	new, relatively small
$p\mathbf{R}$	$4.51\ 10^{-2}$	$7.12\ 10^{-1}$	$8.92\ 10^{-1}$	2.22	new, relatively small

$pp \longrightarrow ppH^+H^-$

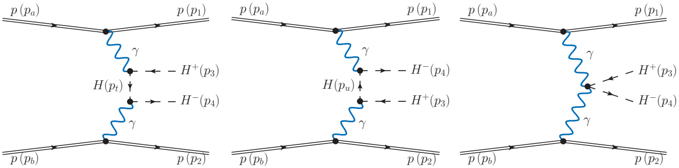

Figure: Born diagrams for exclusive production of pairs of charged scalar particles via photon-photon fusion.

P. Lebiedowicz and A. Szczurek, Phys. Rev. **D91** (2015) 095008.

$pp \to ppH^+H^-$

$$
\begin{aligned}
d\sigma &= \frac{(2\pi)^4}{2s}\overline{|\mathcal{M}_{pp\to ppH^+H^-}|^2}\frac{d^3p_1}{(2\pi^3)2E_1}\frac{d^3p_2}{(2\pi^3)2E_2}\frac{d^3p_3}{(2\pi^3)2E_3}\frac{d^3p_4}{(2\pi^3)2E_4} \\
&\quad \times\delta^4\left(E_a+E_b-p_1-p_2-p_3-p_4\right)\,, \qquad (12)
\end{aligned}
$$

$$
\begin{aligned}
&s=(p_a+p_b)^2, \quad M_{H^+H^-}=p_3+p_4, \\
&t_1=q_1^2, \quad t_2=q_2^2, \quad q_1=p_a-p_1, \quad q_2=p_b-p_2\,. \qquad (13)
\end{aligned}
$$

$$\mathcal{M}^{Born}_{\lambda_a\lambda_b\to\lambda_1\lambda_2H^+H^-}(t_1,t_2) = V^{\mu_1}_{\lambda_a\to\lambda_1}(t_1)D_{\mu_1\nu_1}(t_1)V^{\nu_1\nu_2}_{\gamma\gamma\to H^+H^-}D_{\nu_2\mu_2}(t_2)V^{\mu_2}_{\lambda_b\to\lambda_2}(t_2)\,,$$

$$\begin{aligned} V^{\nu_1\nu_2}_{\gamma\gamma\to H^+H^-} &= V^{\nu_1\nu_2}_t + V^{\nu_1\nu_2}_u + V^{\nu_1\nu_2}_c \\ &= ie^2\frac{1}{p_t^2-m_H^2}(q_2-p_4+p_3)^{\nu_1}(q_2-2p_4)^{\nu_2} \\ &\quad +ie^2\frac{1}{p_u^2-m_H^2}(q_1-2p_4)^{\nu_1}(q_1-p_4+p_3)^{\nu_2} - 2ie^2g^{\nu_1\nu_2}, \end{aligned} \tag{15}$$

$pp \to ppH^+H^-$

$$\mathcal{M}_{pp\to ppH^+H^-} = \mathcal{M}^{\text{Born}}_{pp\to ppH^+H^-} + \mathcal{M}^{\text{absorption}}_{pp\to ppH^+H^-} \,. \tag{16}$$

$$\mathcal{M}^{\text{absorption}}_{\lambda_a\lambda_b\to\lambda_1\lambda_2H^+H^-}(s,\boldsymbol{p}_{1t},\boldsymbol{p}_{2t}) = \frac{i}{8\pi^2 s}\int d^2\boldsymbol{k}_t \mathcal{M}_{\lambda_a\lambda_b\to\lambda'_a\lambda'_b}(s,-\boldsymbol{k}_t^2) \times\mathcal{M}^{\text{Born}}_{\lambda'_a\lambda'_b\to\lambda_1\lambda_2H^+H^-}(s,\tilde{\boldsymbol{p}}_{1t},\tilde{\boldsymbol{p}}_{2t})\,, \tag{17}$$

$pp \to ppH^+H^-$

$m_{H^\pm}$ (GeV)	150	300	500
σ_{LHC} (fb)	0.1474 (0.1132)	0.0119 (0.0080)	0.0014 (0.0008)
σ_{FCC} (fb)	1.0350 (0.9236)	0.1470 (0.1258)	0.0303 (0.0249)

Table: Cross sections in fb for the $pp \to ppH^+H^-$ reaction through photon-photon exchanges without and with (results in the parentheses) the absorption corrections for two center-of-mass energies $\sqrt{s} = 14$ TeV (LHC) and $\sqrt{s} = 100$ TeV (FCC) and various charged Higgs bosons mass values. The calculations was performed for exact $2 \to 4$ kinematics and with the amplitudes in the high-energy approximation.

$pp \longrightarrow ppH^+H^-$

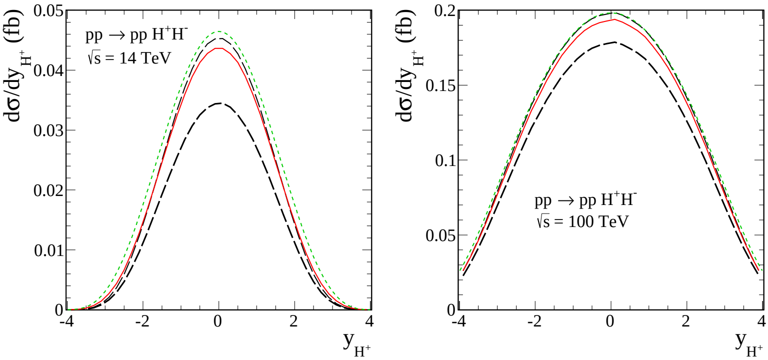

Figure: Rapidity distribution of charged (Higgs) bosons at $\sqrt{s} = 14$ TeV (left panel) and 100 TeV (right panel). The short-dashed (online green) lines represent results of EPA.

$pp \rightarrow ppH^+H^-$

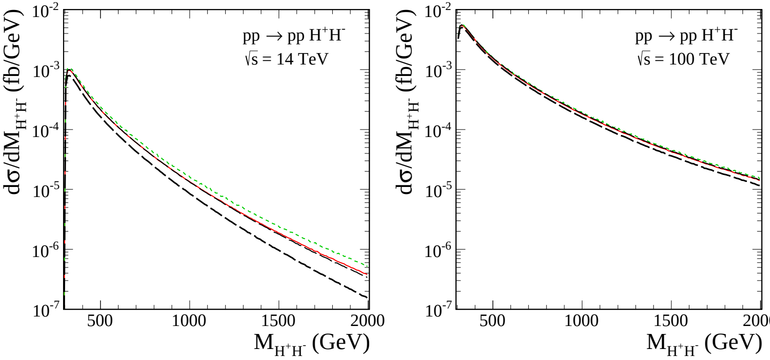

Figure: DiHiggs boson invariant mass distributions at $\sqrt{s} = 14$ TeV (left panel) and 100 TeV (right panel). The short-dashed (online green) lines represent results of EPA.

$pp \to ppH^+H^-$

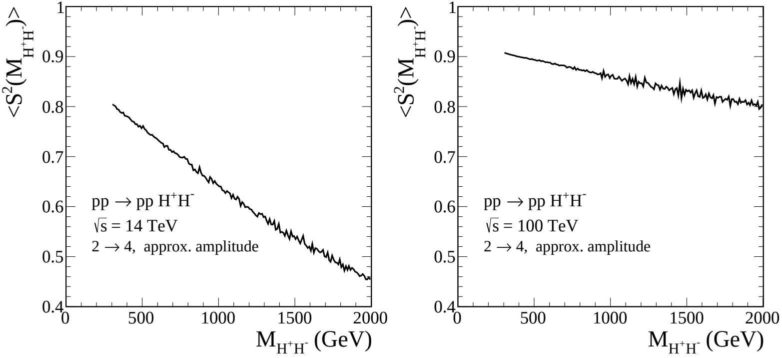

Figure: The dependence of the gap survival factor due to pp interactions on $M_{H^+H^-}$ for exact $2 \to 4$ kinematics at $\sqrt{s} = 14$ TeV (left panel) and 100 TeV (right panel). This is quantified by the ratio of full (including absorption) and Born differential cross sections $\langle S^2(M_{H^+H^-})\rangle$.

$pp \to ppH^+H^-$

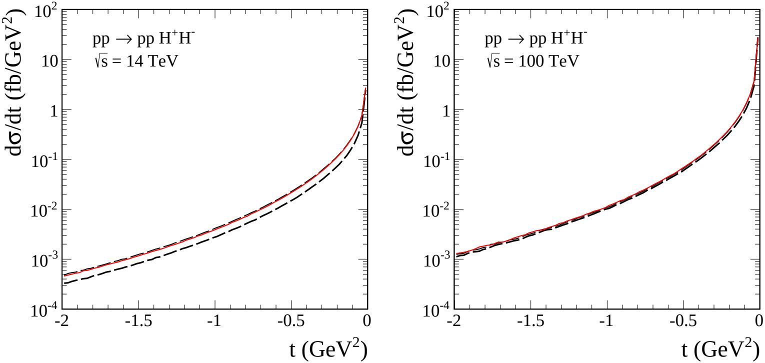

Figure: Distribution in momentum transfer(s) squared (t_1 or t_2) at $\sqrt{s} = 14$ TeV (left panel) and 100 TeV (right panel).

$pp \longrightarrow ppH^+H^-$

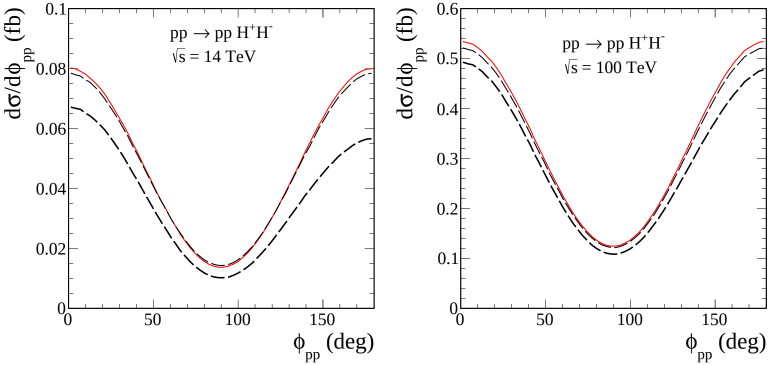

Figure: Distribution in relative azimuthal angle between outgoing protons at $\sqrt{s}$ = 14 TeV (left panel) and 100 TeV (right panel).

$pp \to ppH^+H^-$

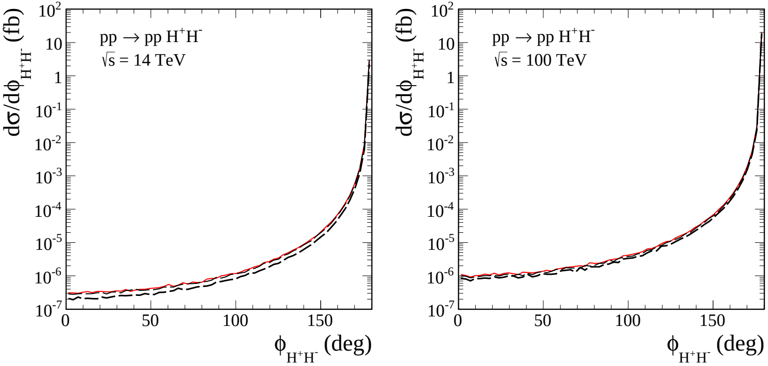

Figure: Distribution in relative azimuthal angle between outgoing charged (Higgs) bosons at $\sqrt{s} = 14$ TeV (left panel) and 100 TeV (right panel).

$pp \to ppH^+H^-$

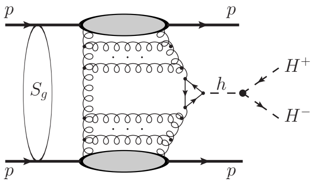

Figure: The diffractive mechanism of the exclusive charged Higgs bosons production through the intermediate *CP*-even neutral recently discovered Higgs boson. The absorption corrections due to *pp* interactions (indicated by the blob) are relevant at high energies.

$pp \to ppH^+H^-$

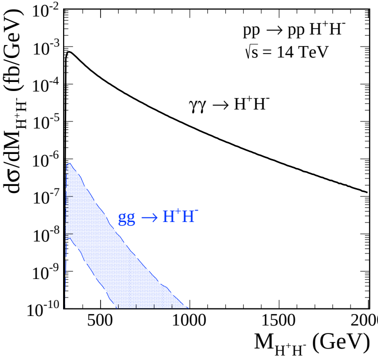

Figure: DiHiggs boson invariant mass distributions at $\sqrt{s} = 14$ TeV (left panel) and 100 TeV (right panel). The upper lines represent the $\gamma\gamma$ contribution. We also show contribution of the diffractive mechanism (the shaded area) for the MSTW08 NLO collinear gluon distribution and $g_{hH^+H^-} = 100$ (1000) GeV for the lower (upper) limit.

$\gamma + \gamma \to \gamma + \gamma$

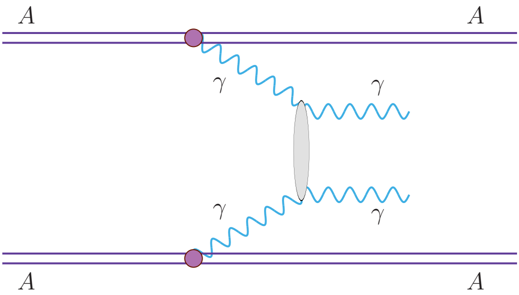

A possibility to study for a first time

$\gamma\gamma \to \gamma\gamma$ reaction

with M. Klusek-Gawenda and P. Lebiedowicz (work in progress)

$\gamma + \gamma \to \gamma + \gamma$

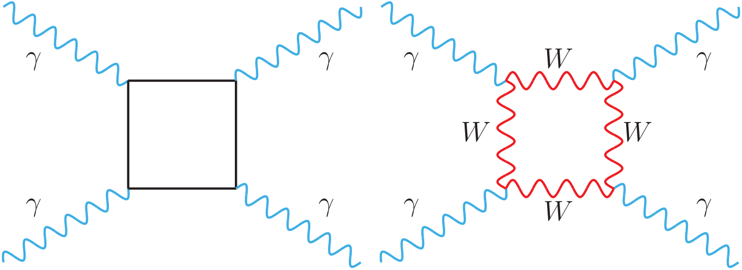

Only Standard Model particles in the boxes

$\gamma + \gamma \to \gamma + \gamma$

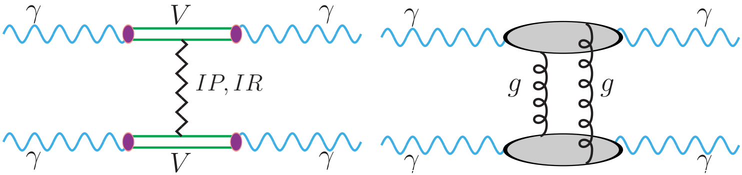

Usually neglected

$\gamma + \gamma \rightarrow \gamma + \gamma$

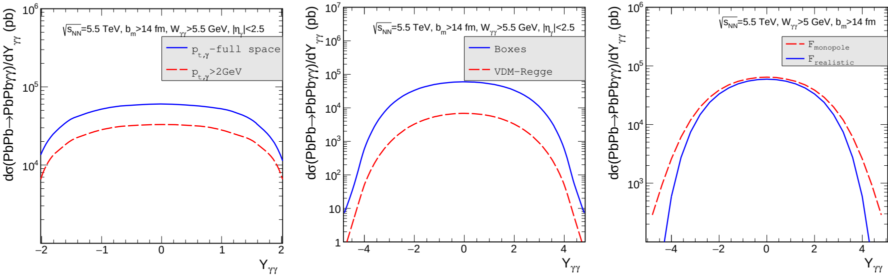

$\gamma + \gamma \to \gamma + \gamma$

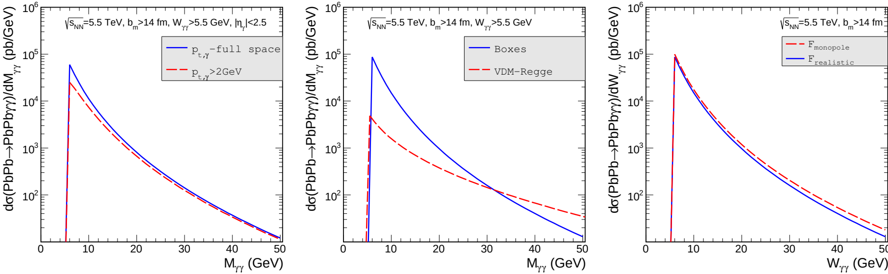

$\gamma + \gamma \rightarrow \gamma + \gamma$

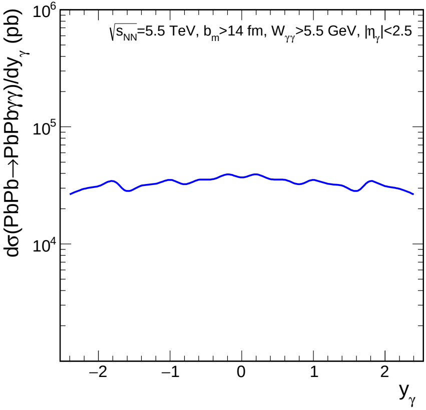

Still not sufficient number of grid points

$\gamma + \gamma \rightarrow \gamma + \gamma$

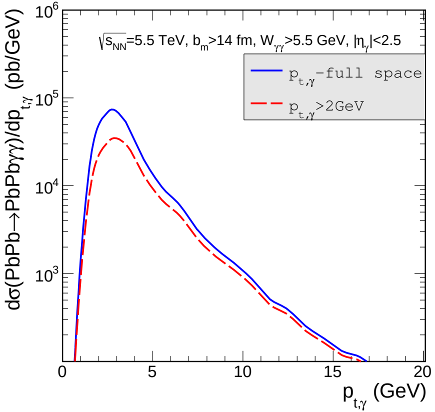

$\gamma + \gamma \rightarrow \gamma + \gamma$

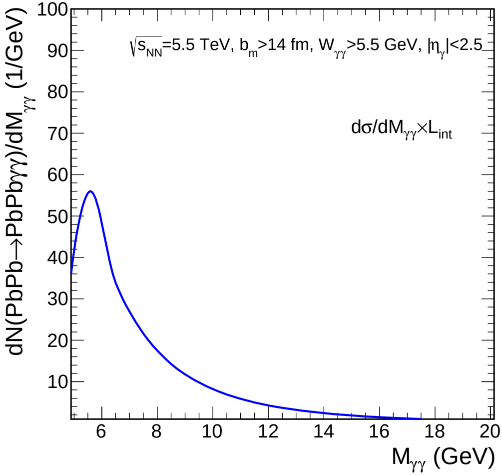

Semi-central collisions

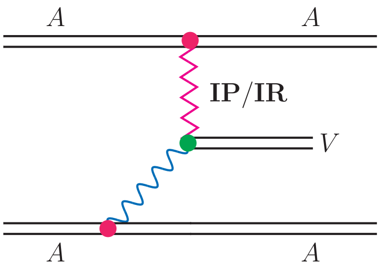

Figure: Schematic diagrams for the single vector meson production by photoproduction (photon-Pomeron (left) or Pomeron-photon (right) fusion.

with M. Klusek-Gawenda (work in progress)

Semi-central collisions

Different mechanisms of J/ψ production in AA collisions

UPC $b > R_A + R_B$	coherent photoproduction (a few studies) p_t - small	incoherent photoproduction (few studies) small multiplicity	
non-UPC $b < R_A + R_B$	coherent photoproduction (new) p_t - small	incoherent photoproduction	NN collisions recomb. in QGP (very popular) huge multiplicity

The incoherent UPC photoproduction has final state which is not fully controlled

How to select the incoherent production ?

Semi-central collisions

Equivalent photon approximation (EPA)

$$\frac{\mathrm{d}\sigma_{A_1A_2\to A_1A_2V}}{\mathrm{d}^2b\mathrm{d}y} = \frac{\mathrm{d}P_{\gamma\mathbf{P}}(b,y)}{\mathrm{d}y} + \frac{\mathrm{d}P_{\mathbf{P}\gamma}(b,y)}{\mathrm{d}y}\,. \tag{18}$$

$$dP_{1/2}(y,b)\,/dy = \omega_{1/2}N(\omega_{1/2},b)\,\sigma_{\gamma A_{2/1}\to VA_{2/1}}(W_{\gamma A_{2/1}})\,, \tag{19}$$

Two contributions added incoherently.

Semi-central collisions

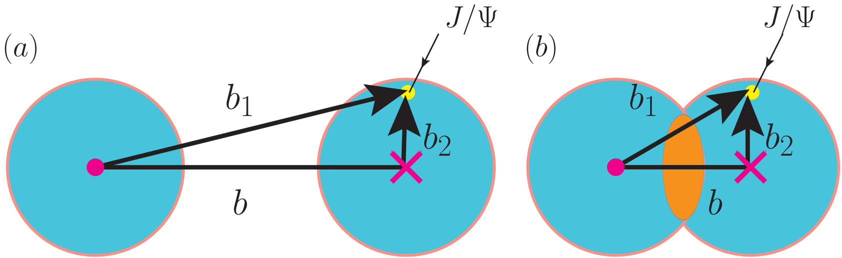

Figure: Impact parameter picture of the collision and the production of the J/ψ meson for ultraperipheral (left panel) and for semi-central (right panel) collisions. It is assumed here that the first nucleus is the emitter of the photon which rescatters in the second nucleus being a rescattering medium.

Semi-central collisions

A model for the cross section:

$$\frac{\mathrm{d}\sigma\left(\gamma p \to J/\psi p; t=0\right)}{\mathrm{d}t} = b_{J/\psi} X_{J/\psi} W_{\gamma p}^{\epsilon_{J/\psi}} \,, \tag{20}$$

$$\frac{\mathrm{d}\sigma\left(J/\psi p \to J/\psi p; t=0\right)}{\mathrm{d}t} = \frac{f_{J/\psi}^2}{4\pi\alpha_{em}} \frac{\mathrm{d}\sigma\left(\gamma p \to J/\psi p; t=0\right)}{\mathrm{d}t} \,, \tag{21}$$

$$\sigma_{tot}^2\left(J/\psi p\right) = 16\pi \frac{\mathrm{d}\sigma\left(J/\psi p \to J/\psi p; t=0\right)}{\mathrm{d}t} \,, \tag{22}$$

$$T_A\left(\mathbf{r}\right) = \int \rho\left(\sqrt{r^2+z^2}\right)\mathrm{d}z \,, \tag{23}$$

$$\frac{\mathrm{d}\sigma\left(\gamma A \to J/\psi A; t=0\right)}{\mathrm{d}t} = \frac{\alpha_{em}\sigma_{tot}^2(J/\psi A)}{4f_{J/\psi}^2} \,. \tag{24}$$

Semi-central collisions

Important ingredient:

Classical mechanics

$$\sigma_{tot}^{CM}\left(J/\psi A\right) = \int \mathrm{d}^2\mathbf{r}\left(1 - \exp\left(-\sigma_{tot}\left(J/\psi p\right) T_A\left(\mathbf{r}\right)\right)\right) \ , \qquad (25)$$

Quantum mechanics (Glauber)

$$\sigma_{tot}^{QM}\left(J/\psi A\right) = 2\int \mathrm{d}^2\mathbf{r}\left(1 - \exp\left(-\frac{1}{2}\sigma_{tot}\left(J/\psi p\right) T_A\left(\mathbf{r}\right)\right)\right) \ , \qquad (26)$$

Semi-central collisions

Flux modifications:

$$N^{(1)}(\omega_1, b) = \int N(\omega_1, b_1)\, \frac{\partial(R_A - \mathbf{b_2})}{\pi R_A^2} \mathrm{d}^2 b_1 \ , \tag{27}$$

$$N^{(2)}(\omega_1, b) = \int N(\omega_1, b_1)\, \frac{\partial(R_A - \mathbf{b_2}) \times \partial(\mathbf{b_1} - R_A)}{\pi R_A^2} \mathrm{d}^2 b_1 \ . \tag{28}$$

Semi-central collisions

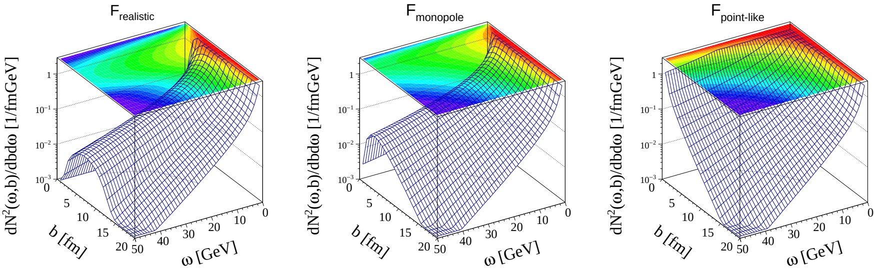

Figure: Standard photon fluxes calculated for realistic (left panel) monopole (middle panel) and point-like (right panel) form factor.

Semi-central collisions

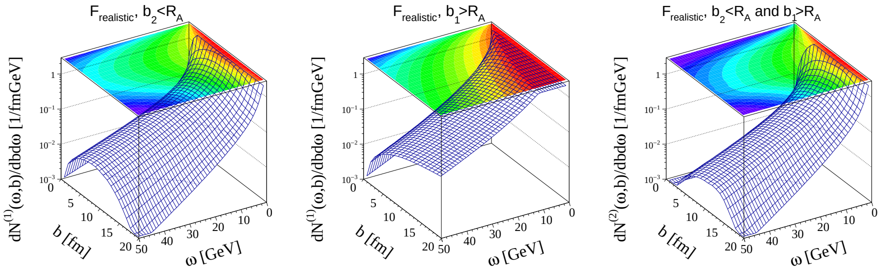

Figure: Two-dimensional distributions of the photon flux in the impact parameter b and in the energy of photon ω. Three figures are for three different photon flux approximation.

Semi-central collisions

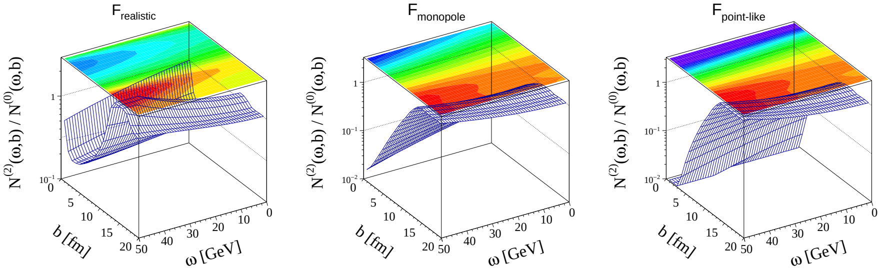

Figure: The ratio of the differential photon fluxes in the impact parameter b and energy of the photon ω. The left panel shows the case with the realistic form factor. The middle figure relates to monopole form factor and the right panel shows the ratio when the point-like form factor is taken into account.

Semi-central collisions

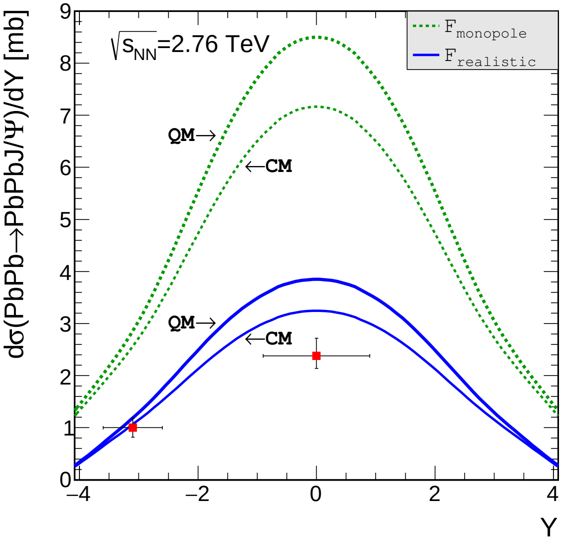

Semi-central collisions

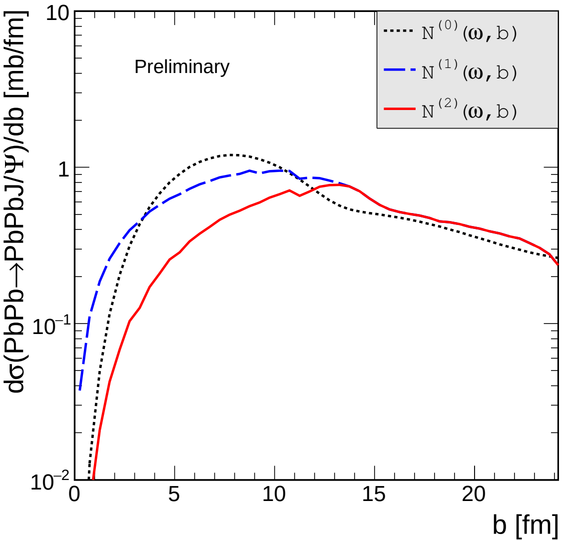

Semi-central collisions

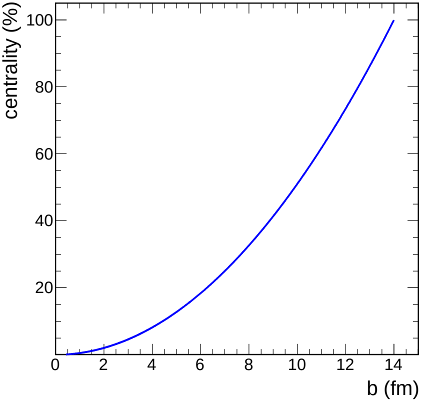

Figure: Centrality of nuclear collisions as a function of the impact parameter.

Semi-central collisions

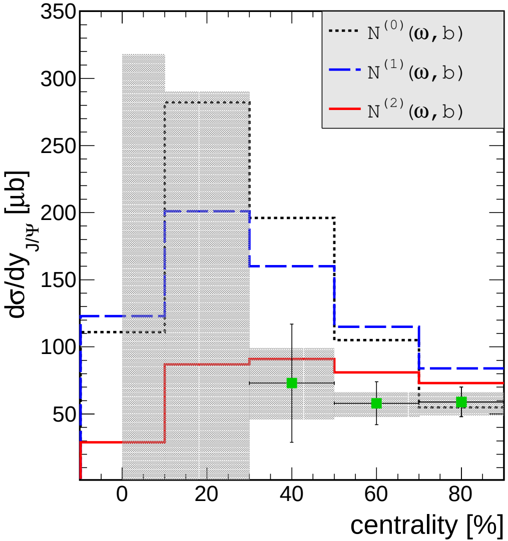

Semi-central collisions

Summary of total cross sections

- realistic form factors
- $\sqrt{s_{NN}} = 2.76$ TeV
- full rapidity range

UPC	16.32 mb
non-UPC, $N^{(0)}$	10.08 mb
non-UPC, $N^{(1)}$	9.38 mb
non-UPC, $N^{(2)}$	5.48 mb

The same order of magnitude !!!

Now time for hard work

See you in two years